Directing towards structural insights into the α2β2 isoform of the Na,K-ATPase and the effect of FXYD7

Master Thesis

Sabrina Krepel

Rijksuniversiteit Groningen, 2021

Structural insights into the α2β2 isoform of the Na,K-ATPase and the effect of FXYD7

Sabrina Tirtsa Krepel

Second master thesis

Student number: S2380837

Biomolecular Sciences

Daily supervisor: Michael Habeck*

Examiners: Poul Nissen*
Dirk Slotboom‡

Laboratory of Structural Neurobiology

Aarhus University

March 2021

*Laboratory of Structural Neurobiology, Aarhus University

‡Laboratory of Structural Membrane Biology, Rijksuniversiteit Groningen

Contents

Abstract

The Na,K-ATPase establishes an electrochemical gradient of Na- and K-ions over the plasma membrane of a large number of tissues, including the heart, kidney and brain. The properties of the Na,K-ATPase are adjusted accordingly by varying the isoform assembly of its subunits alpha, beta and accessory subunit FXYD. The combination of α1β1 is most common and present in all tissues where α2β2 is found predominantly in muscle cells and astrocytes. The disfunction of α2β2 has been connected to brain-related conditions such as Familial Hemiplegic Migraine (FHM) and Rapid-onset Dystonia Parkinsonism (RDP). α2β2 has a low K^+-affinity, steep voltage sensitivity and is significantly less stable than α1β1. The question remains how these differences are established. In this study, α2β2 Na,K-ATPase was expressed in *Pichia pastoris*, purified and reconstituted in Saposin A nanodiscs and stabilized with MgF_x and ATP in an E2 conformation. Structural analysis by negative stain electron microscopy resulted in a promising dataset with visible subunit domains, but cryo-EM of the same sample did not extend this into a high-resolution map. ATPase assays of this sample showed that α2β2 is significantly less stable in KCl compared to NaCl during purification, which was largely due to the absence of Na^+ rather than the presence of KCl. Cryo-EM of α2β2 purified in the presence of both NaCl and KCl, stabilized with MgF_x and ATP with additional lipids during washes showed a slight improvement of the dataset. Additionally, due to the stabilizing nature of FXYD proteins and reported cross-linking of α2β2 to FXYD7, FXYD1 and FXYD7 were compared in terms of stabilization and inhibition by MgF_x. FXYD7 stabilized α2β2 during purification in the same manner as FXYD1 but decrease in activity after purification was virtually identical between α2β2 without or with any FXYD, reflecting the general instability of the isoform. In summary, this study shows that the α2β2 isoform combination of human Na,K-ATPase can be subjected to structural studies by cryo-EM, although additional modification of the purification procedure and grid preparation is necessary to accommodate for stability differences compared to the more commonly studied α1β1 isoform. Furthermore, it is necessary to elaborate on studies regarding the effect of FXYD7 on α2β2 and possibly extend this to other isoforms and consider other regulatory roles of FXYD7 for the Na,K-ATPase in general.

Introduction

Maintaining an ionic gradient

One of the most important mechanisms that has been adopted by multicellular organisms to advance in their evolution is to adapt to extra- and intracellular ionic concentration gradients and use it to their advantage. The integrity of the cell structure, as well as the inherent functions of numerous enzymes are dependent on the intracellular chemical conditions, including concentrations of sodium, potassium, calcium and many other ions[1]. Moreover, concentration gradients of some ions are used to exert specific functions in the body, creating a basis for a whole array of processes essential for bodily function. The discovery of the Na,K-pump in 1957 by Jens Christian Skou has been paramount to understanding these mechanisms and earned him a Nobel prize in 1997[2,3]. Initially recognized as an ATPase, it is now known that the Na,K-pump engages in active transport of sodium and potassium ions across the plasma membrane to create an ionic concentration gradient, that can be utilized by all mammalian tissues in different manners[4]. In kidney, the highly expressed Na,K-ATPase creates and maintains the gradient for filtering blood and reabsorbing glucose and other nutrients[5], while in various brain cells, the Na,K-ATPase takes up a significant amount of energy to establish the gradient needed to fire action potentials in neurons[6].

With the Na,K-pump present in virtually all kinds of mammalian tissues, a number of diseases and complications have been connected to disfunction of the protein. Mutations in the Na,K-ATPase can lead to problems with the heart[7,8], but many have also been identified in neurological diseases including Alternating Hemiplegia of Childhood (AHC)[9], Rapid-onset Dystonia Parkinsonism (RDP)[10], Alzheimer's Disease[11,12] and Familial Hemiplegic Migraine (FHM)[13]. Some pharmacological applications have been developed using cardiac glycosides, which are natural inhibitors of the Na,K-pump[14]. Cardiac glycosides have been applied in treatments for heart complications, by indirectly raising cytoplasmic calcium levels via the sodium-calcium exchanger, enhancing the contractability of the heart[15]. Other pharmacological approaches that include the Na,K-pump have also been suggested, including anti-tumour therapeutics[16].

Structural and biochemical properties of the Na,K-ATPase

The Na,K-pump is part of the P-type ATPase superfamily, characterized by their ability to hydrolyse ATP while transporting different substrates, such as ions, uphill across the membrane[17]. In the case of the Na,K-pump, 3 Na-ions are transported to the outside of the plasma membrane and 2 K-ions to the inside per cycle. A functional Na,K-ATPase consists of two main domains (α and β). ATP is hydrolysed by the combined actions of the cytoplasmic domains, consisting of the actuator (A), phosphorylation (P) and nucleotide-binding (N) domain (Figure 1A). These domains combined with 10 transmembrane helices compose the α-subunit of the oligomeric Na,K-pump. The β-subunit serves another function as a chaperone and regulatory domain[18]. Together, they form a basis of the oligomeric complex that designates the Na,K-pump, with different isoform combinations resulting in varying characteristics, such as ion-affinity and stability, on which will be elaborated below. Additionally, an accessory FXYD subunit can further direct the functionality of the protein. With this wide range of possibilities, specific Na,K-pump isoforms are found in different tissues, according to their characteristics[19].

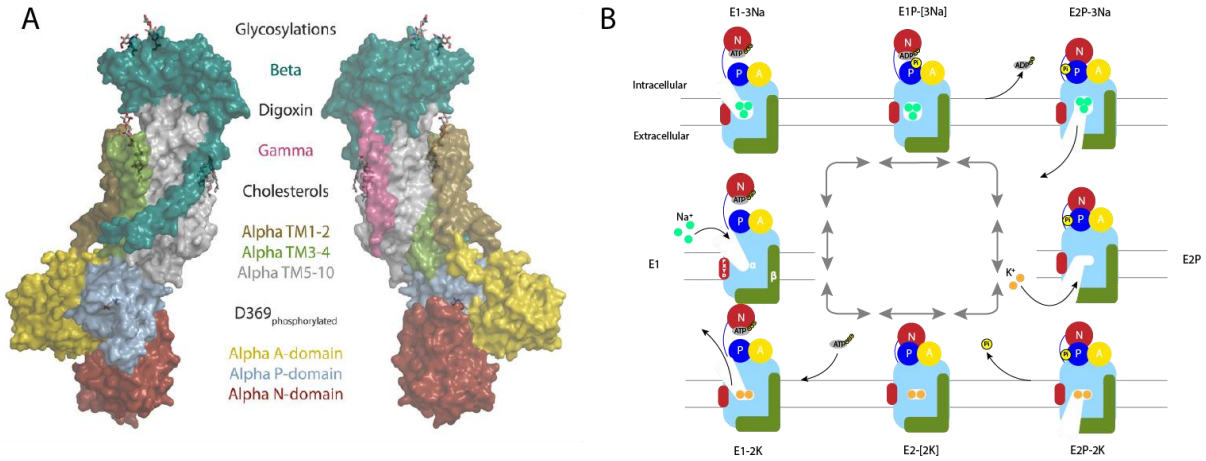

Figure 1 Structural features and mechanism of the Na,K-ATPase. ***A.*** *Structure of the digoxin-stabilized α1 isoform from pig kidney[20] (PDB: 4RET), adapted from Clausen et al.[4]. Glycosylations, digoxin, cholesterol and the phosphorylated aspartate are shown as sticks.* ***B.*** *Post-Albers cycle of the Na,K-ATPase, in which three Na-ions are transported to the extracellular space and 2 K-ions to the intracellular side. The α-subunit is depicted in light blue, the β-ectodomain in green, FXYD in red and the A/N/P-domains are indicated. Na-ions are depicted in light-green and K-ions in orange.*

The transportation of ions is the result of switching between two main conformations E1 and E2, also referred to as the Post-Albers cycle[21–23] (Figure 1B). E1 describes the conformation in which the affinity for Na-ions is elevated, and E2 increases affinity for K-ions. In between these conformations, there are different phases describing the transition. When ATP is bound to the E1 conformation, transmembrane helix 1 moves up to make room for 2 Na-ions to bind, compensated by negative charges from residues within the transmembrane domain. Phosphorylation of a conserved aspartate residue in the P-domain by ATP drives a conformational change, in which E1 transitions to E2 by occluding the ions, release of ADP and release of the three Na-ions on the extracellular side. Poulsen and colleagues proposed that a cytoplasmic proton promotes Na-ion release by occupying site III[24]. Because the aspartate stays phosphorylated during this transition, these states are also designated E1P and E2P, respectively. In E2P, two K^+-ions can bind from the extracellular space upon which the ions are occluded and subsequently released in the cytoplasm while the aspartate in the P-domain is dephosphorylated. ATP can bind again and release of the proton from site III together with the two K^+-ions from site I and II signifies transition into an E1 state.

Isoform specificities and regulation of the Na,K-ATPase

As the human Na,K-ATPase comes in different subunit isoforms, the preference for ions can be adjusted by combining the subunits in specific manners. There are four α-subunit isoforms (α1-4), which can be combined with three different β-subunits (β1-3)[4]. The most common combination is α1β1, which can be found in practically all human tissues with elevated concentrations in heart and kidney[5,25,26]. Because α1β1 is essential for viability, it is improbable that mutations leading to loss of function result in a viable phenotype. Mutations in α1 have, however, been connected to an altered hormone balance in aldosterone producing adenomas[27]. Other alpha-isoforms are less common in the human body, with α2 primarily present in astrocytes and in heart and skeletal muscle[28,29], α3 in neuronal projections and dendritic spines[30] and α4 specifically in spermatozoa[31,32].A number of mutations have been identified that can lead to an array of diseases, ranging from neurological dysfunction such as Familial Hemiplegic Migraine (FHM2) caused by α2 mutations and Alternating Hemiplegia of Childhood (AHC) and Rapid-onset Dystonia Parkinsonism (RDP) related to α3 mutations, to male infertility caused by α4 mutations. Therefore, insights into these isoforms may prove useful for future pharmaceutical research, extending the only current application involving cardiotonic steroids inhibiting the Na,K-ATPase in heart treatment[15].

Adding to the variability of biochemical properties of the Na,K-ATPase, beta-isoforms can further adjust the affinity of the protein to Na- or K-ions[18]. Although it is presumed that there are more common combinations of certain alpha-isoforms with certain beta-isoforms[33,34], any combination results in a functional protein when expressed in *Xenopus* oocytes[35]. A functional beta-subunit consists of one transmembrane helix, a N-terminal cytoplasmic tail, and a C-terminal ectodomain. Three pump-stabilizing disulfide bonds[36] and a conserved Y(Y/F)PYY motif are the distinct features of the beta subunit. It has been proven to be of importance for several neurological functions such as sight and hearing in *Drosophila*[37] and motor functions in mice[38,39]. In humans, gliomas have been connected to altered expression patterns of β2[40]. The three beta-isoforms share less sequence identity with each other than alpha-isoforms and further distinguish themselves by differences in the number of glycosylation sites (3 for β1, 8 for β2 and 2 for β3) and the possibility of glutathionylation of a cysteine in the transmembrane part of β1 in response to oxidative stress[41].

Whereas the alpha- and beta-subunit form the minimal basis of a functional Na,K-ATPase, another single-helix regulatory subunit is often associated with it. Among its 7 isoforms, FXYD proteins derive their name from a common PFxYD motif in the extracellular N-terminal domain and share two common conserved glycine residues and a serine residue[42,43]. Most isoforms appear to lower ion affinity of the Na,K-ATPase, in favour of their tissue-specific function. Because FXYD proteins are widely expressed and have a significant effect on the Na,K-ATPase, it is important to take their role into account when studying the full protein. Moreover, mutations in the FXYD2 gene have been connected to hypomagnesemia in humans[44]. FXYD1 has been found to significantly stabilize the Na,K-ATPase[45], which is a desirable feature when studying the purified protein.

Na,K-ATPase isoforms in research: α2β2 as a subject of interest

There are some discrepancies in the amount of information available per isoform. Relatively, a lot of information has been elucidated on the general properties and structural features of the α1β1 isoform, whereas other combinations have not been studied thoroughly. Not only can this be explained by the fact that this isoform combination is well represented in the body, but its inherent thermostable feature is also suited for research purposes. However, the lethality of loss-of-function mutations signifies a small chance of disease phenotypes that are associated with α1β1. A study of α2 with its preferred beta-subunit β2[33] in the heart and brain may be of interest to gain more insight into physiological properties of the Na,K-ATPase in general and pharmacological applications, specifically since β2 has the strongest effect on the functional properties of the Na,K-ATPase out of all β isoforms by reducing the K-ion affinity[35]. This difference has been attributed to a difference in TM helix tilt compared to the other beta-isoforms[39], but this is not conclusive. Next to this, α2 exhibits a higher sensitivity to voltage[46], perfectly suiting the α2β2 protein complex for rapid extracellular K^+-clearance and thereby protecting from depolarization in neurons. Indeed, a list of mutations has been connected to Familial Hemiplegic Migraine (FHM), a condition that expresses itself in attacks during which subjects experience aura and weakness on one side of the body. Studies on the Na,K-ATPase α2β2 protein in astrocytes indicate that FHM may be caused by an increase in extracellular K-ion and glutamate concentration, which leads to an increase of cortical spreading depression. Because α2β2 in astrocytes contributes directly to extracellular K^+-clearance and indirectly to extracellular glutamate clearance[47], disfunction of α2β2 results in an increase of cortical spreading depression[48,49]. Next to the importance of α2β2 in the brain, it has also been found that α2 has a higher affinity for cardiotonic steroids in the heart, supporting the hypothesis that treatment of heart failure with cardiotonic steroids may be beneficial because of their effect on α2 isoforms rather than α1 isoforms. Therefore, increasing our understanding of this specific complex can broaden the possibilities for drug treatments and our general understanding of human molecular processes.

A number of structures are available of the Na,K-ATPase, although none of them concern a human isoform. Nevertheless, many structural insights can be derived from structures of pig kidney[20,50–52] or shark salt gland[53–55] Na,K-ATPase, most of them bound to cardiotonic steroids and/or metal fluorides, stabilizing E1 and E2 states. Some features about the mechanism of gating are assumed by comparing to a similar protein, SERCA1a[56,57]. These structures provide a lot of information on the general mechanism that the Na,K-ATPase adopts, but do not elucidate the structural basis of how the isoforms adjust the biochemical properties of the protein. Recent advances in electron microscopy have made it possible to overcome issues that presented themselves when attempting crystallization of membrane proteins[58]. With this in mind, obtaining structures of human Na,K-ATPase isoforms may be in reach, finally shining light on how the alpha and beta subunits have such an impact on the properties of all isoforms.

FXYD7 as an additional focus for α2β2

Although the focus of researching Na,K-ATPase regulation has largely been on the beta-subunits, FXYD interactions are also of importance to the functionality of the protein complex. In many studies, FXYD1 is used to stabilize the Na,K-ATPase, as it is the most widely expressed FXYD in the body[42]. Differences between the effect of FXYD isoforms on the Na,K-ATPase have been studied[43], but these studies have also limited themselves to α1β1. Especially since α2β2 malfunction in astrocytes is a disease-relevant subject, FXYD proteins expressed in the nervous system, such as FXYD7[59], might offer a chance to better understand he regulation of α2β2 in the brain. Although α2β2 does not associate with FXYD7 when expressed in *Xenopus* oocytes, recent mapping of protein interactions in the brain via crosslink mass spectrometry (XL-MS)[60] has found an association between α2 and FXYD7. Since FXYD7 decreases external K^+-affinity regardless of external Na^+ concentration, while the activity overall is more sensitive to inhibition by external Na^+, FXYD7 is suggested to play an important role in preventing an extracellular K^+-undershoot after neuronal activity[42]. Therefore, the combination of α2β2 with FXYD7 would be a logical tool for astrocytes to engage in neuronal K^+-clearance. Considering that FXYD1 significantly enhances thermostability of α1β1, it may be advantageous to study if FXYD7 has the same effect on α2β2.

Research techniques of Na,K-ATPase studies

To study the α2β2 complex, it is necessary to equip the right tools to express, purify and analyse the protein. Expression of the Na,K-ATPase has previously been successfully performed in *Pichia pastoris*[33,45], using an expression system based on methanol utilization[61,62]. The principle is based on the ability of the organism to switch to a metabolism in response to methanol being the only carbon source present, for which peroxisomal alcohol oxidases AOX1 and AOX2 are greatly expressed to convert methanol to formaldehyde and hydrogen peroxide. AOX1 plays the most prominent role in alcohol oxidase activity, accounting for 90% of total activity and 30% of total protein weight[63]. Because of the high amount of protein produced in presence of methanol, the *AOX1* promotor can drive expression of recombinant Na,K-ATPase genes by replacing the coding sequence of AOX1 with the coding sequence of Na,K-ATPase by homologous recombination, while retaining the promotor and termination regions of AOX1. In the exponential growth phase, methanol is added to be the only carbon source available in the medium, resulting in a relatively high expression of His_{10}-tagged Na,K-ATPase, which can be subsequently purified from membranes with Immobilized Metal Affinity Chromatography (IMAC).

Because membrane proteins can be challenging to purify without aggregation and native conditions are not approached when solubilized in detergent, a commonly used technique is the use of nanodiscs[64–66]. There are several different nanodiscs in use, but they all share the common feature of being able to solubilize a membrane protein while maintaining the phospholipid bilayer integrity,

forming a disc around the complex. Another advantage is the fact that lipid composition is easier to be monitored, and, in contrast with liposome reconstitution, the chemical conditions on both sides of the membrane do not change over time during activity assays. Lastly, the nanodisc concept is a perfect match with single-particle cryo-EM, in which high quality single particles must be picked in order to construct a high resolution structure[67]. Nanodisc formation using Saposin proteins has been proven to be beneficial in structural studies[68] and reconstitution of the Na,K-ATPase in Saposin A has been performed and optimized previously (data not published).

Lastly, it is essential to create a homogenous sample to properly classify particles with electron microscopy. Therefore, stabilization of domains with compounds is common in structural biology in general and the Na,K-ATPase is no exception. Because cardiotonic steroids are natural high-affinity inhibitors of the Na,K-ATPase, they are regularly used to stabilize the protein in the E2P conformation. Next to this, a regularly used group of stabilizing agents for the Na,K-ATPase are metal fluorides, such as MgF_x or AlF_x. These compounds can mimic phosphate groups, therefore preventing phosphoryl transfer in the Post-Albers cycle. The versatile nature of metal fluorides can cause the protein to be stabilized in various conformations, enabling production of homogenous particles for (cryo-)EM. Therefore they are helpful compounds to gain insights into structural features of the Na,K-ATPase.

Project objective

In order to gain more insight into the structural features of Na,K-ATPase isoform complex α2β2, an attempt will be made to produce cryo-EM samples of Saposin A-reconstituted Na,K-ATPase in a E2 state to study the structural basis for differences in K^+-affinity. Expression, purification and stabilization of α2β2 will be a central subject, further analysed by ATPase activity assays and NanoDSF analysis. An additional focus will be on the accessory subunit FXYD7, primarily accentuating the question whether it will further stabilize α2β2 and/or differentiate the properties of the protein in terms of ATPase activity compared to the commonly used FXYD1.

Materials and methods

Expression and purification of Saposin A in *E. coli*. *E. coli* strain Rosetta gami-2 (DE3) with isopropyl β-d-1-thiogalactopyranoside (IPTG) inducible vector pNIC28-Bsa4 was used to express Saposin A protein. The strain was grown at 37 °C in Terrific Broth (TB) medium (2% w/v lysogeny broth (LB), 2% w/v yeast extract (YE), 70 mM KP_i pH 7.4, 0.8% glycerol, 6µg/ml tetracycline, 25µg/ml kanamycin and 17µg/ml chloramphenicol). Expression cultures were inoculated at OD_{600} of 0.1 and grown to OD_{600} of 0.5-0.6 before induction with 1 mM IPTG overnight at 20 °C. Cells were harvested by centrifugation at 6000 rpm for 15 minutes and pellets were flash frozen and stored at -80 °C for further use. To lyse the cells, pellets were resuspended in 40 mL lysis buffer (20 mM MOPS/Tris pH 7.4, 150 mM NaCl, 50 mM Imidazole and 1 mM PMSF) per 10 g of cells and sonicated 3x 5 minutes at 60% amplitude 1 second off/1 second on with 5 minutes cooling in between cycles. Lysate was centrifuged for 20 minutes at 5000g, after which the supernatant was heated to 85 °C in a heat block for 10 minutes. The sample was subsequently centrifuged at 22,000g for 30 minutes and incubated for 1 hour with Ni^{2+}-resin beads (1 mL/10 g cells). The beads were loaded on a gravity column and washed 3x with 2 bead volumes wash buffer (20 mM MOPS/Tris pH 7.4, 150 mM NaCl and 5 mM imidazole). Saposin A was eluted in 5 fractions of 1 bead volume with elution buffer (20 mM MOPS/Tris pH 7.4, 150 mM NaCl or other salt and 200 mM imidazole). Protein containing fractions were identified by Bradford (BioRad protein assay) and pooled to be dialyzed overnight with a 5 kDa cut-off membrane against dialysis buffer (20 mM MOPS/Tris pH 7.4, 150 mM NaCl or other salt when indicated) with Tobacco Etch Virus (TEV) protease 1:100 w/w to remove the His-tag. The dialyzed sample was run through the same Ni^{2+}-resin column and washed with 1 bead volume of dialysis buffer. Protein concentration was determined by nanodrop and concentrated to 10-25 mg/mL with a 5 kDa cut-off concentrator before a 15-minute ultracentrifugation (100,000g) and loading on a Superdex 200 16/600 column equilibrated with dialysis buffer. Fractions containing monomeric Saposin A were pooled and diluted to 1 mg/mL, flash frozen and stored at -80 °C for further use.

Fermenter expression of Na,K-pump in *Pichia pastoris*. On the basis of methanol induction in *P. pastoris* for protein expression, a pre-existing strain SMD1165 of *P. pastoris* was used that harbours the respective Na,K-ATPase sequence with flanking AOX1 promotor sequence in the 5' direction and AOX1 terminating sequence in the 3' direction. The respective strain was streaked on a yeast-extract peptone dextrose (YPD) medium agar plate (1% yeast extract, 2% peptone, 0.3% glucose, 2% agar) and incubated at 30 °C for 2-3 days. Subsequently, 10 mL buffered minimal glycerol (BMG) medium with added yeast nitrogen base (YNB) and biotin (100 mM KPi pH6, 0,3% glycerol, 0,34 g/L YNB, 10 g/L ammonium sulfate, 0,4 mg/L biotin) was inoculated with a single colony and incubated at 30 °C for 2 days. According to OD, a respective volume was used to inoculate 100 mL BMG medium to grow for 18-22 hours. This culture was subsequently used to inoculate 5L BMG with YNB and biotin in a benchtop fermenter (BioFlo II, New Brunswick Scientific). Cells were grown to OD 8 in a glycerol batch phase, followed by a semi exponential fed-batch phase to grow until OD 25-30 with 40% glycerol feeding solution stirred at 300 rpm/min at 30 °C, aerated with compressed air at 5 L/min. 15% ammonium hydroxide solution was attached to the fermenter at a constant flow rate to maintain a pH of 5. At OD 25-30, the temperature was lowered to 25 °C (α1 isoforms) or 22 °C (α2 isoforms). After one hour, a final concentration of 0.35% methanol was added to induce, which was repeated after 12 hours. Cells were harvested at 6000 rpm for 10 minutes 16-18 hours after induction and the pellet was flash frozen and stored at -80 °C.

Membrane preparation. Cell pellets (60-90 g) were resuspended in lysis buffer (40 mM MOPS/Tris pH 7.4, 1 M sorbitol and 1 mM EDTA) to a total volume of ~180 mL. Phenylmethylsulfonyl fluoride (PMSF) was added to a final concentration of 1 mM. The following steps are all performed under cooling

conditions (on ice or 4 °C). Cells were lysed by bead beater for 5x 1.5 minutes with 1.5 min intervals for cooling using an equal volume of 0.5mm glass beads. Lysate was adjusted to 400 mL with lysis buffer and centrifuged for 20 minutes at 8,000g to separate unbroken material and the supernatant was ultracentrifuged at 100,000g for 90 minutes. Pellets were resuspended and homogenized with a glass homogenizer in 20 mM MOPS/Tris pH 7,4 to a final volume of 40 mL. 10 mL 10 M urea was added dropwise and incubated for 20 min. Sample was diluted to ~180 mL using the same buffer and ultracentrifuged as before. Pellets were resuspended to a final concentration of 300 mg/mL (wet weight) in resuspension buffer (20 mM MOPS/Tris pH 7,4, 20% glycerol, 1 mM PMSF, 5µg/ml leupeptin, 5µg/ml chymostatin and 5µg/ml pepstatin). Membranes were flash frozen and stored at -80 °C until further use.

Purification of Na,K-pump in detergent. All steps are performed under cold conditions. Membranes were thawed on ice and diluted to 90 mg/mL (total wet weight) in 20 mM MOPS/Tris pH 7,4, 200 mM NaCl, KCl or choline chloride, 30 mM imidazole, 10% glycerol, 1 mM PMSF and 0.6% w/w *n*-Dodecyl β-D-maltoside (DDM) and 0.06% w/w cholesterol hemisuccinate (CHS) for solubilization. The sample was sonicated at 50% amplitude, 1 sec on 1 sec off, for 1 minute before centrifugation at 100,000g for 30 minutes. Supernatant was incubated with 0.4 mL Talon cobalt beads (per 2 g membrane starting material or 100 mg membrane protein) for 4 hours while tilting. Afterwards, beads were spun down and 90% supernatant was removed before adding 25 µg FXYD per gram membrane protein and incubated overnight. Beads were again spun down after incubation and washed in batch with 10 bead volumes of wash buffer (20 mM MOPS/Tris pH 7,4, 10% glycerol, 200 mM KCl, NaCl or choline chloride, 30 mM imidazole, 0.3 mg/mL C12E8 and lipids (0.1 mg/mL 1-stearoyl-2-oleoyl-*sn*-glycero-3-phosphoserine (SOPS), 0.07 mg/mL L-α-phosphatidylcholine from soy (SoyPC) and 0.05 mg/ml cholesterol)). Beads were loaded on a gravity column and washed with 5 additional bead volumes wash buffer. Protein was subsequently eluded in 4 fractions of 0.5 bead volume elution buffer (wash buffer + 200 mM imidazole). Protein concentration was determined by Bradford assay (BioRad protein assay).

Purification of Na,K-pump in Saposin A. Purification with the intent of reconstitution in Saposin A was done in the same manner as in detergent for the first part but diverges after overnight incubation with FXYD protein. The beads were then washed in batch with 5 bead volumes wash buffer without lipids (20 mM MOPS/Tris pH 7,4, 10% glycerol, 200 mM KCl/NaCl or choline chloride and 0.3 mg/mL C12E8). Beads were loaded on a gravity column and washed with 5 additional bead volumes of wash buffer without lipids before transfer to a 2 mL Eppendorf tube with 400 µL relipidation buffer (20 mM MOPS/Tris pH 7,4, 10% glycerol, 200 mM KCl/NaCl or choline chloride with 0.3 mg/mL C12E8 and lipids (0.16 mg/mL SOPS, 0.16 mg/mL SoyPC and 0.05 mg/ml cholesterol supplemented with relevant inhibitors) per 400 µL beads. The protein was incubated for 20 minutes before addition of 500µg Saposin A per 0.4ml Talon beads and incubated for another 20 minutes. The beads were loaded on a gravity column and washed 2x 2 bead volumes with wash buffer 2 (20 mM MOPS/Tris pH 7,4, 10% glycerol, 200 mM KCl/NaCl or choline chloride and 30 mM Imidazole). The reconstituted protein was eluted in 4 fractions of 0.5 bead volume with elution buffer (wash buffer 2 with 250 mM Imidazole and relevant inhibitors). Eluted protein concentration was determined by Bradford assay. Fractions containing protein were pooled and concentrated with a 5 kDa cut-off concentrator (Vivasoin) to a volume <500 µL to be spun down (100,000g for 15 minutes) and loaded on a Superdex 200 Increase 10/300 GL column. Relevant fractions were pooled and used for activity assays or loaded on a grid for electron microscopy.

ATPase activity assay using the PK/LDH coupled enzyme assay. To measure protein activity, a PK/LDH coupled enzyme assay was used that is based on NADH absorbance (340 nm). In a 96-wells plate, 10

µL inhibitor or water was combined with 80 µL mastermix (final concentration 20 mM MOPS/Tris pH 7.4, 120 mM NaCl, 20 mM KCl, 1 mM EGTA, 3 mM $MgCl_2$, 5 mM phosphoenolpyruvate (PEP), 0.6 mM nicotinamide adenine dinucleotide (NADH), 0.0092 mg/mL pyruvate kinase (PK), 0.0226 mg/mL lactate dehydrogenase (LDH) and protein (0.004 mg/mL) if applicable). For heat incubations, concentrated protein was placed on a heat block and samples were taken and placed on ice at respective time points. The plate was incubated for 10 minutes at 37 °C before addition of 10 µL ATP (final concentration 1 mM) to start the reaction. Absorbance of NADH was monitored on a plate reader (SpectraMax i3, Molecular Devices) at 340 nm for 30-50 minutes at 37 °C. The slope was used to calculate protein ATPase activity.

Preparation of negative stain grids. Gilder G400 mesh copper grids were used and coated with colloidon before adding an amorphous carbon layer with a carbon evaporator. Grids were stored in a dry environment for further use. When preparing a sample, grids were glow discharged for 30s at 25 mA before adding 3 µL sample and incubating for 30s, after which the grid was blotted by touching Wattman filter paper with the side of the grid. In some cases, the grid was washed three times by facing down the grid in a droplet of deionized water and blotting on the filter paper in between. The sample was subsequently stained 3 times with 3 µL uranyl formate, drying the grid the same way on filter paper in between addition of uranyl formate. Grids were left to dry for a few minutes and stored in a dry environment before analysis on a Tecnai Spirit electron microscope.

Preparation of cryo-grids. Preparation of a Na,K-ATPase sample for cryo-EM was done in a similar fashion as a normal purification with Saposin A reconstitution, with a few changes. 700 mg of membrane protein were used as starting material, diluted with the same buffer conditions. DDM/CHS was added dropwise during homogenization in a glass homogenizer. The purification protocol was subsequently followed, upscaling Talon bead volume to 2.8 mL and relative amounts of FXYD were adjusted to the starting material (700 µL of 1 mg/mL). Beads were washed in batch with 10 mL wash buffer without or with lipids (0.1 mg/mL SOPS, 0.02 mg/mL cholesterol), washed on a gravity column with 10 mL of the same wash buffer. Relipidation (450 µg SOPS, 450 µg SoyPC, 140 µg cholesterol in 2.8 mL 20 mM MOPS/Tris pH 7,4, 10% glycerol, 200 mM KCl or 200 mM NaCl+10 mM KCl with 0.3 mg/mL C12E8 and inhibitor (4 mM $MgCl_2$, 20 mM KF, 1 mM ATP)) was divided over 5 fractions and incubated while rotating for 20 min before addition of 700 µL Saposin in respective buffers (KCl or NaCl). After 20 min, beads were loaded on 5 gravity columns, washed 2x 1 mL wash buffer (20 mM MOPS/Tris pH 7,4, 10% glycerol, 200 mM KCl or 200 mM NaCl+30 mM KCl) and eluted in 6 fractions of 200 µL with the same buffer + 200 mM Imidazole. Protein containing fractions were pooled and dialyzed twice with a 3.5 kDa cut off membrane against 500 mL dialysis buffer (20 mM MOPS/Tris pH 7.4, 200 mM KCl or 120 mM NaCl +30 mM KCL, 10% glycerol, 1 mM $MgCl_2$ and 0.1 mM DTT) for two hours. Protein was concentrated to ~400 µL and run on a Superdex 200 Increase 10/300 size exclusion column. Relevant fractions were pooled and concentrated to 0.7 mg/mL. Inhibitor was added (4 mM $MgCl_2$, 20 mM KF and 1 mM ATP) and LMNG was added (1.5x CMC, 0.015 mg/mL) and sample was put on C-flat 1.2/1.4 400 mesh copper grids and plunge frozen in liquid ethane with a Vitrobot (100% humidity, 4 °C, various blotting times). Grids were analysed on a Titan Krios electron microscope by the Embion facility.

Data processing of (cryo-)EM datasets. Micrographs for negative stain grids were taken on a Tecnai Spirit electron microscope, using Leginon software[69]. In general, approximately 200 micrographs were taken at 69,000x magnification at varying defocus values between 0.8-2 µm. This typically resulted in a particle count of 150,000-200,000, which were further processed using *cis*TEM[70] and cryoSPARC[71]. 3D maps that resulted from processing were visualized in Chimera. For cryo-EM datasets, data processing was done solely in *cryo*SPARC.

Expression and purification of FXYD proteins. FXYD was expressed in *Escherichia coli* BL21 bearing an IPTG inducible vector for human FXYD1 or FXYD7. LB medium (10 g/L NaCl, 10 g/L tryptone, 5 g/L yeast extract) with kanamycin was inoculated with an overnight culture, grown at 37 °C and at OD_{600}=0.6 induced with 0.5mM IPTG. After expression overnight at 18°C, cells were harvested and washed with wash buffer (50 mM MOPS/Tris, pH 7.4, 500 mM NaCl, 1 mM EDTA, 1 mM PMSF). Cells were lysed by sonication (3x 5 min at 50% intensity with 1 sec on 1 sec off and 5min cooling between cycles) before a centrifugation step (200,000xg for 30 min at 4 °C). Cell pellets containing inclusion bodies were subsequently solubilized in solubilization buffer (20 mM MOPS/Tris, pH 7.4, 10% glycerol, 500 mM NaCl, 5 mM Imidazole, 8M urea and 4 mg/mL DDM) in 15 mL/g pellet and incubated at room temperature for one hour. After diluting urea to 6M, sample was centrifuged at 200,000xg for 30 min at 4 °C. Supernatant was incubated with cobalt beads (0.5 mL beads/g pellet) for one hour and subsequently spun down (500xg 2 min at 4 °C) to remove unbound material. Beads were washed in batch with 5 bead volumes wash buffer (20 mM MOPS/Tris pH 7.4, 10% glycerol, 500 mM NaCl, 5 mM Imidazole, 4M Urea and 1 mg/mL DDM), loaded on a gravity column and washed with 5 additional bead volumes wash buffer. FXYD was eluted in 5 fractions of 1 bead volume with elution buffer (20 mM MOPS/Tris pH 7.4, 10% glycerol, 500 mM NaCl, 200 mM Imidazole, 4M urea and 0.3 mg/mL DDM). FXYD containing fractions were pooled and flash frozen and stored at -80 °C for further use. Pooled fractions were dialyzed overnight against 100x volume dialysis buffer (20 mM MOPS/Tris pH 7.4, 10% glycerol, 500 mM NaCl, 0.1 mM DTT) with a 3.5 kDa cut off membrane. Tev-protease was added in a 1:10 w/w ratio with 1 mM DTT and left at RT for 7 hours. Cleaved FXYD was loaded on the same column used previously for reverse IMAC. Concentration of the flowthrough was measured and diluted to 1 mg/mL in dialysis buffer, aliquoted in 500 µL fractions and stored at -80 °C for further use.

Results

Purification and reconstitution of the Na,K-ATPase in Saposin A nanodiscs. Previously, Na,K-ATPase has been expressed and purified using the *AOX1* expression system, which yielded functional protein without any indication of toxicity to the host[45]. For this study, solubilization of membrane proteins followed by His_{10}-tag purification resulted in relatively pure α2β2 yield, both in detergent (Figure 2A) as well as reconstituted in Saposin A (Figure 2B). Generally, 2000 mg of wet weight membrane yielded 40-50 µg α2β2 Na,K-ATPase in detergent. When purified with NaCl in purification buffers, detergent-solubilized α2β2 exhibited varying ATPase activity within a range of 6-11 µmol/mg/min. Following a Hill-kinetics curve (n=2.65), ATPase activity could be inhibited by titration with metal fluoride MgF_x, formed by combining varying amounts of KF and a constant amount of $MgCl_2$ in the activity mixture (Figure 2C). Size exclusion chromatography of reconstituted α2β2 resulted in a profile in which peaks could be clearly separated, showing an initial void peak, and peaks containing dimeric or monomeric Na,K-ATPase (Figure 2D).

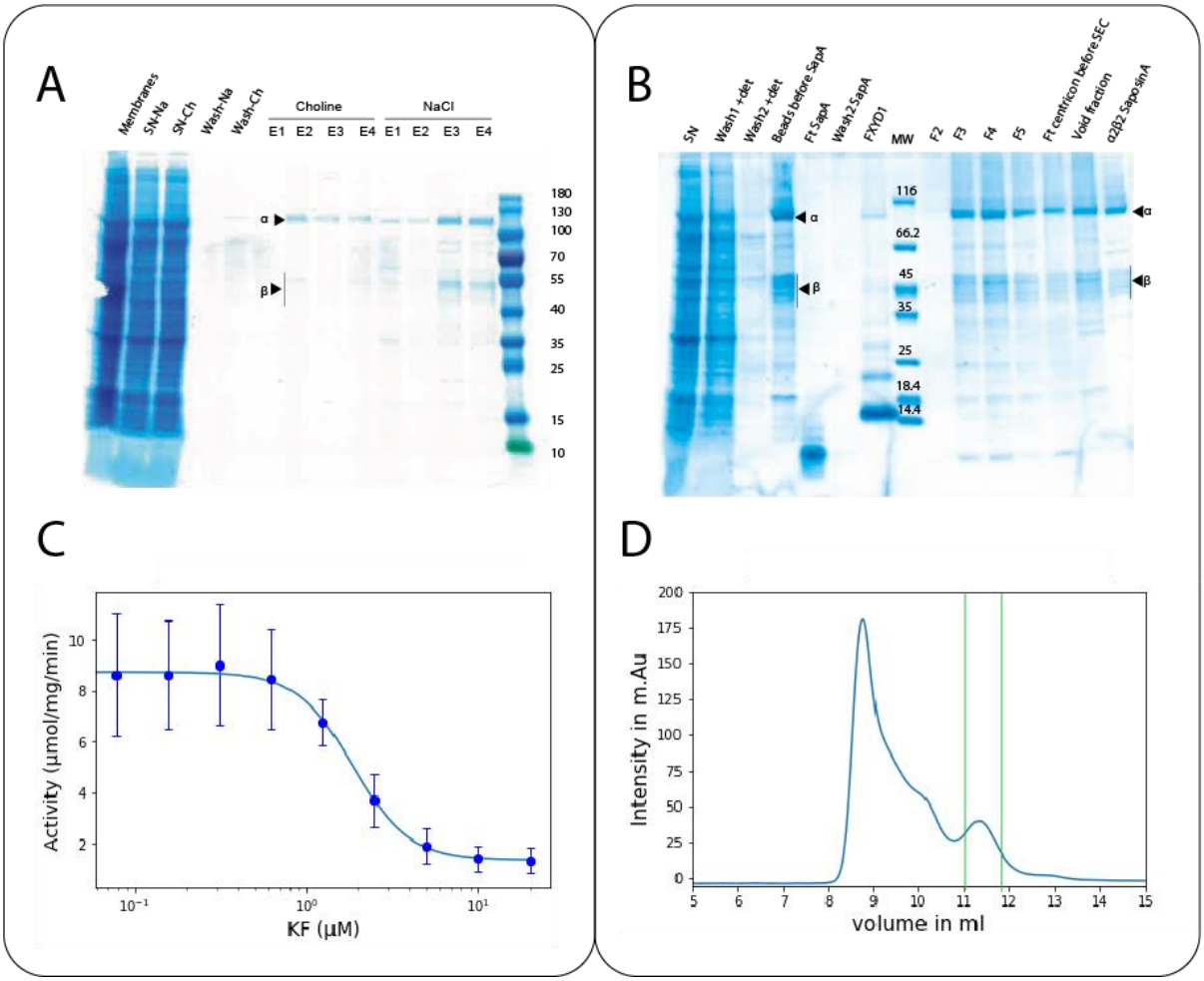

Figure 2 Purification of α2β2 and reconstitution in Saposin A. ***A.*** *Visualization on a 4-20% SDS polyacrylamide gel of solubilization and purification in detergent, in which solubilization was done in buffers containing NaCl and subsequent purification in either NaCl or choline chloride. Beta subunits appear as scattered lines with varying molecular weight due to differences in glycosylation. (SN = supernatant, Na = NaCl, Ch = choline chloride, EX for respective elution fractions)* ***B.*** *Similar visualization of purification and reconstitution of α2β2 in Saposin A nanodiscs. (SN = supernatant, det = detergent, SapA = Saposin A, MW = Molecular Weight, FX for respective size exclusion fractions, ft = flowthrough, SEC = size exclusion chromatography)* ***C.*** *Titration of KF (MgF_x) for NaCl-purified α2β2 in detergent resulting in a Hill-curve with* n *= 2.65, V_{max}= 8.74 µmol/mg/min and $K_{0.5}$= 1.87 mM. D. Size exclusion profile of α2β2 reconstituted in Saposin A nanodiscs, with a void peak (~8.7 mL), a dimer peak (~10.3 mL), and a peak containing monomeric α2β2 (~11.5 mL).*

Reconstituted α2β2 in Saposin A nanodiscs supplemented with 20 mM KF results in a comprehensive 3D map from negative stain data. Following purification and reconstitution of α2β2 in Saposin A nanodiscs, the possibility of creating negative stain data was explored with the addition of 20 mM KF, which would result in a 4-5 mM MgF_x concentration, corresponding to a complete inhibition of α2β2 ATPase activity. Additionally, a sample was prepared with AlF_x instead of MgF_x, to assess any differences in quality between metal fluoride inhibited samples. The addition of MgF_x or AlF_x was to stabilize the cytoplasmic alpha domains in a E2 conformation. A dataset of micrographs was collected with Leginon on a Tecnai spirit microscope at 69,000x magnification with a defocus range of 0.8 -2 µm. Compared to the AlF_x sample, classified particles of the MgF_x sample appeared more homogenous, resembling expected features of reconstituted Na,K-pump, with the nanodisc, the A/N/P-domains of the alpha-subunit and the beta C-terminal domain on the extracellular side clearly visible (Figure 3B). Following this 2D classification, selected classes were subjected to a 3D classification, generating a low resolution envelope that resembled previous E2-state Na,K-pump structures of the α1β1 isoform (Figure 3C). Although the particles of α2β2 were of high quality under the microscope with negative stain, ATPase activity measurements of α2β2 in detergent purified in 200 mM KCl showed that the sample did not exhibit ATPase activity under measured circumstances, whereas the protein was active when purified in 200 mM NaCl (Figure 4B). This difference was also reflected when analysed by NanoDSF, where detergent-solubilized α2β2 purified in KCl showed a decrease in thermal stability compared to NaCl, respectively (Figure 4A). Therefore, although particles purified in KCl yielded a promising 3D map with negative stain, a lack of ATPase activity might raise a question as to whether the sample reflects the *in vivo* structure of α2β2.

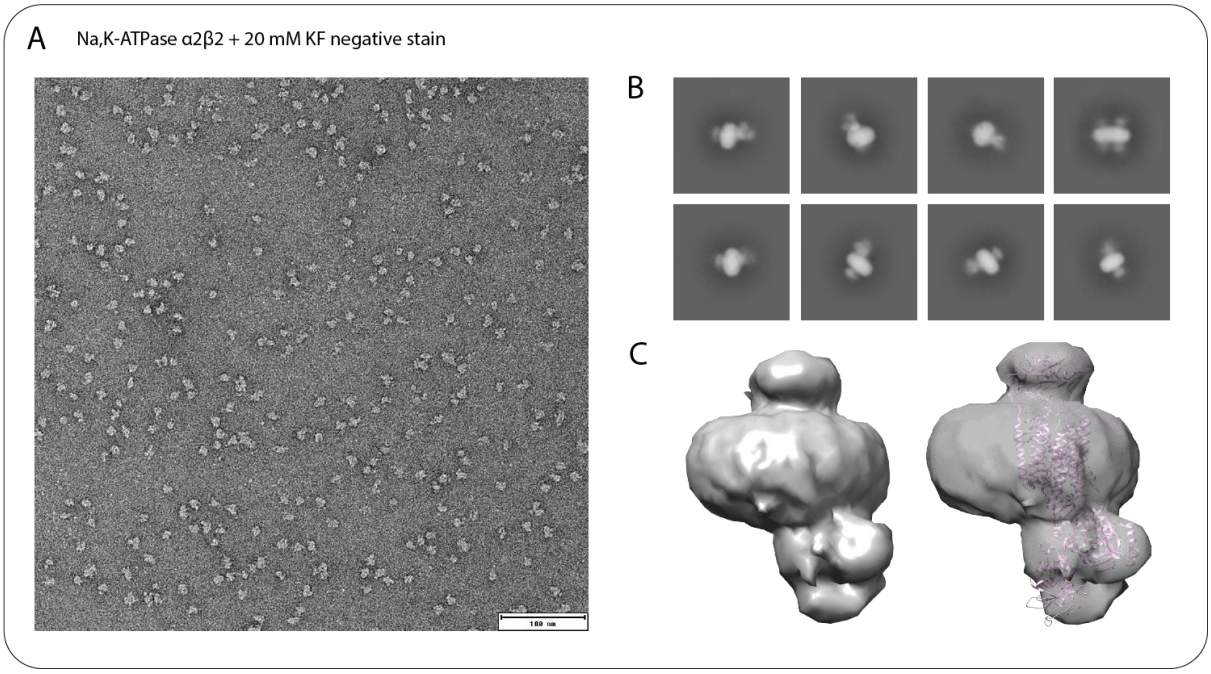

*Figure 3 Negative stain of α2β2 reconstituted in Saposin nanodiscs **A.** Exemplary microcraph of α2β2 with 20 mM KF (4-5 mM MgF_x), taken at 69,000x magnification and -1.5 µm defocus. **B.** Particles were taken from micrographs and subjected to 2D classifications using CryoSparc, which resulted in 2D classes with visible nanodisc, cytoplasmic α-domains and β- ectodomain. **C.** 3D ab initio modelling resulted in low resolution map in which the different domains are visible. A structure of shark salt gland E2-MgF_x (PDB: 2ZXE) was fitted in the map and showed a similar shape. Map constructed with CryoSparc and visualized in Chimera.*

Purification of detergent-solubilized α2β2 in choline chloride did not result in ATPase activity comparable to NaCl. The instability of α2β2 Na,K-ATPase when purified in KCl is a remarkable, yet unexpected feature. Although the initial objective of structural studies on the E2-conformation of α2β2 was to gain more insight as to why the K^+-affinity is lowered compared to α1β1, an additional subject of interest is to clarify the structural basis of the observed instability differences. Because α2β2 exists in the E1 state when purified in high NaCl concentration and the E2 state when purified in high KCl concentration, the difference in stability indicates that stability is dependent on the state of the protein. To assess the influence of Na- and K-ions, α2β2 was purified with high-concentration choline chloride and low-concentration KCl. Choline chloride provides high ionic strength for stability during purification but does not occupy any binding sites. However, the Na,K-ATPase is generally stabilized in an E1 conformation by high ionic strength, therefore a low amount of KCl (20 mM) is added to push the protein to an E2 conformation with bound K-ions. Although ATPase activity of α2β2 solubilized in detergent improved when purified in choline chloride, the activity did not match NaCl-purified sample (Figure 4B). The inhibition curve of MgF_x did not significantly change (Figure 4C). This observation may indicate a stability dependency on Na-ions occupying the Na-binding sites, rather than instability resulting from KCl presence. However, KCl might play a role in decreasing thermal stability off α2β2. Samples purified in choline chloride with added KCl should contain α2β2 in E2 state, which is also the case when it is purified in high KCl-concentration. Therefore, the difference in activity can only be attributed to the difference in KCl concentration. It is important to take this effect on ATPase activity into account when analysing the structure of α2β2 in nanodiscs by (cryo-)EM.

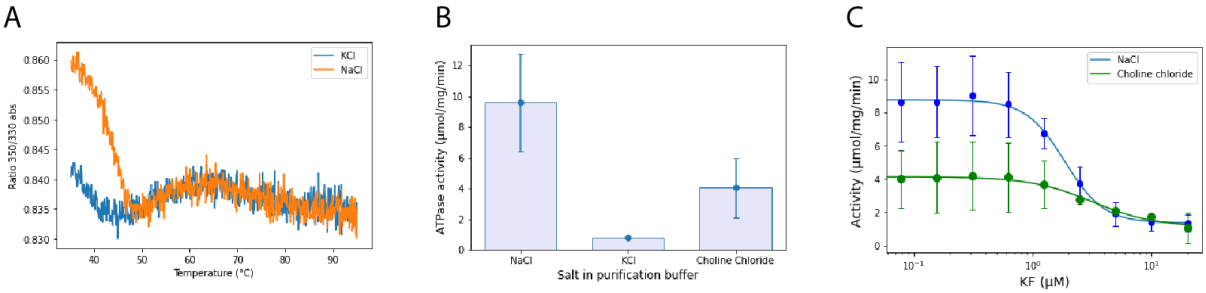

Figure 4 Stability of detergent-solubilized α2β2 in different salts. ***A.*** *NanoDSF profiles reflecting the 350/330 emission ratio of α2β2 in detergent purified in KCl (blue) or NaCl (orange) over a temperature range of 35°C to 95°C.* ***B.*** *Activity of detergent-solubilized α2β2 purified in NaCl, KCl or choline chloride.* ***C.*** *KF (MgF_x) titration of detergent-solubilized α2β2 purified in NaCl or in choline chloride. (NaCl: V_{max}= 8.74 µmol/mg/min $K_{0.5}$= 1.87 mM, choline chloride: V_{max}= 4.13 µmol/mg/min, $K_{0.5}$= 3.20 mM, n = 1.64)*

Cryo-EM of α2β2 reconstituted in nanodiscs and purified in KCl resulted in a poor sample of which particles could not be classified in 2D classes resembling a Na,K-pump. Although (thermo)stability issues seemed to arise when detergent-solubilized α2β2 was purified in KCl, negative stain data of the same sample reconstituted in Saposin A nanodiscs provided a positive outlook for cryo-EM studies of α2β2 under these circumstances. Therefore, a cryo-EM dataset was recorded of reconstituted α2β2 purified in the same conditions using a Titan Krios2 electron microscope (Figure 5A). The 2D classes that resulted from this action did not resemble a Na,K-pump, possibly showing broken particles. The observed negative stain data therefore did not necessarily translate into clear cryo-EM data. It is important to note that sample preparation for negative stain takes less time compared to cryo-EM sample preparation, with a difference of several hours. This result, in combination with the observation that α2β2 seems to decrease in thermal stability when purified in KCl, led to the decision to make a sample suitable for cryo-EM purified in 200 mM NaCl with 30 mM KCl added with MgF_x and ATP to stabilize the E2 conformation.

Cryo-EM of α2β2 reconstituted in Saposin A nanodiscs and purified in 200 mM NaCl with 30 mM KCl resulted in a better, but not ideal dataset. Because purification of α2β2 reconstituted in Saposin A nanodiscs in high KCl did not result in a comprehensive dataset, another attempt was made to improve the particle quality and homogeneity. The instability of α2β2 in high KCl concentration was taken into account, thus a sample was made with 200 mM NaCl for ionic strength and 30 mM KCl to provide K-ions. The amount of MgF_x (4-5 mM) and ATP (1 mM) remained the same, which should stabilize the protein in the E2 state regardless of the excess of Na-ions present. Replacing the KCl with NaCl should provide a more stabilizing environment, according to the activity and stability measurements done previously. Another alteration to the procedure to enhance stability of the protein was the addition of lipids to the wash buffers, further reducing the amount of time in which there are no lipids present that can stabilize the protein[72]. With these alterations, 300-mesh copper cryo-grids were made of α2β2 in Saposin A and analysed on a Titan Krios2 electron microscope (Figure5B). The 2D classes generated from this dataset seemed to resemble protein particles better than the previous dataset, but further optimization was needed to provide higher quality datasets. One observation that could be made was a possible orientation bias for a top/bottom view, which was not observed before for structures of α1β1, which generally shows a side-view preference. The conclusion that could be drawn from this dataset consisted of the necessity to screen more conditions for purification of the sample, blotting conditions or other inhibitors such as cardiac glycosides.

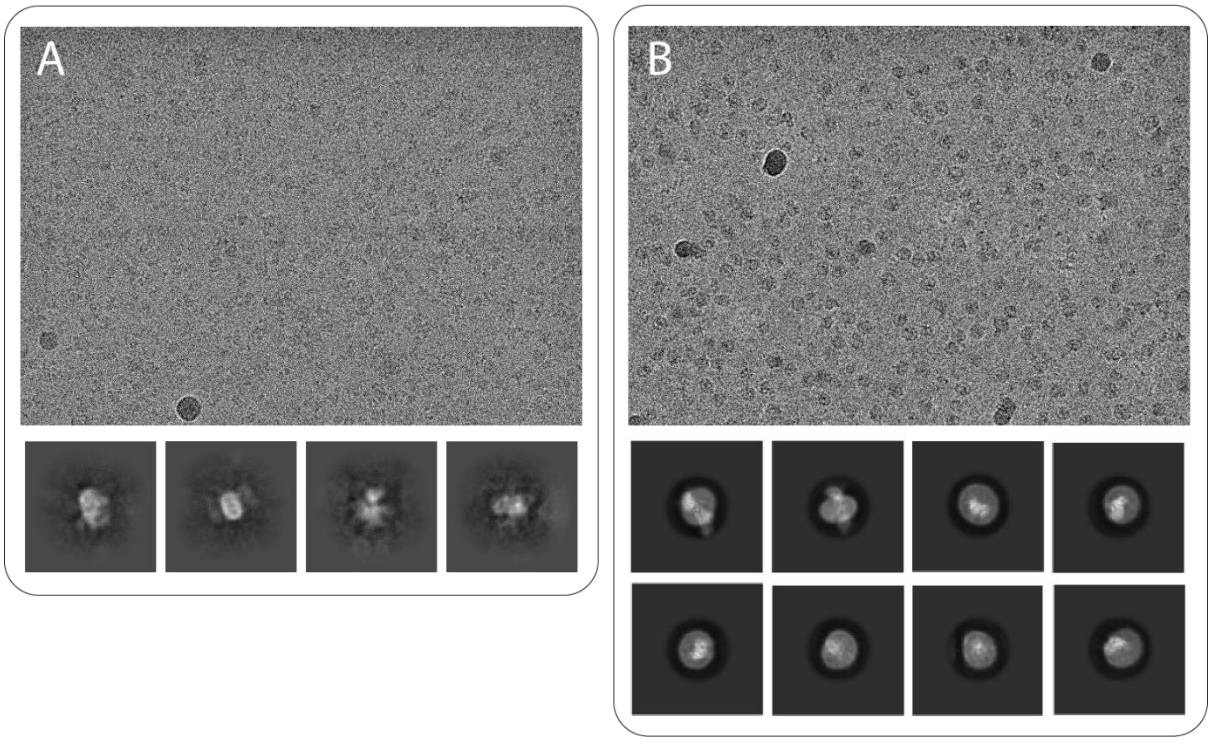

*Figure 5 Cryo-EM of α2β2 in E2*K2 conformation stabilized by 4-5 mM MgF_x and 1 mM ATP.* ***A.*** *Micrograph of the first cryo-EM sample, which was purified with high concentration KCl and no lipids in wash buffers (69,000x magnification, taken on a Titan Krios2 electron microscope by the EMBION facility of Aarhus University). Data processing resulted in 2D classes shown.* ***B.*** *Micrograph of the second cryo-EM sample, which was purified with high NaCl concentration and added lipids during washes.*

FXYD7 does not change the ATPase activity or stability of α2β2 in detergent. FXYD proteins are known to stabilize the Na,K-ATPase during purification, next to their regulatory role. In a recent study, α2 in the brain has been suggested to interact with FXYD7, which is expressed solely in the nervous system[59]. To investigate the effect of FXYD7 on α2β2 stability and activity, FXYD7 was purified and added instead of FXYD1 during the purification procedure. ATPase activity assays were performed in

detergent solubilized α2β2, with either FXYD1, FXYD7, or no FXYD added during purification. Initial MgF_x titration curves showed a very similar inhibition of α2β2 with FXYD7 ($K_{1/2}$ = 1.42 mM, V_{max} = 10.84 µmol/mg/min) to α2β2 with FXYD1 ($K_{1/2}$ = 1.30 mM, V_{max} = 10.95 µmol/mg/min, Figure 5A). With no FXYD present during purification, a reduction in initial activity is observed, while no change in inhibition occurs. It was already known that FXYD1 stabilizes the Na,K-ATPase during purification[44], which therefore explains the reduction of activity of α2β2 without FXYD ($K_{1/2}$ = 1.40 mM, V_{max} = 7.66 µmol/mg/min). Although previous studies noticed an evident stabilization of α2β1 by FXYD1 when incubated at 37°C, coupled enzyme activity assays of α2β2 show a 2-fold faster decrease in ATPase activity and no significant difference between samples with or without FXYD (Figure 5B). The activity of the three respective samples was also monitored over a time frame of three days, in which a reduction was observed due to the inherent instability of α2β2 (Figure 5C). Although stabilization of α2β2 by FXYD1 or FXYD7 is evident from initial activity assays, percentual decrease in total ATPase activity over the following three days was virtually the same (Figure 5D). This observation indicates that for α2β2, FXYD mainly stabilizes the protein during purification and the effect is less apparent after purification. What is more, significant differences in stabilization between FXYD1 and FXYD7 are not evident from the ATPase assays performed, although more data are needed in order to draw conclusions from these assays. It is important to note that the PK/LDH coupled enzyme assay does not distinguish between turnover rate and total activity and is therefore merely an indication of stability.

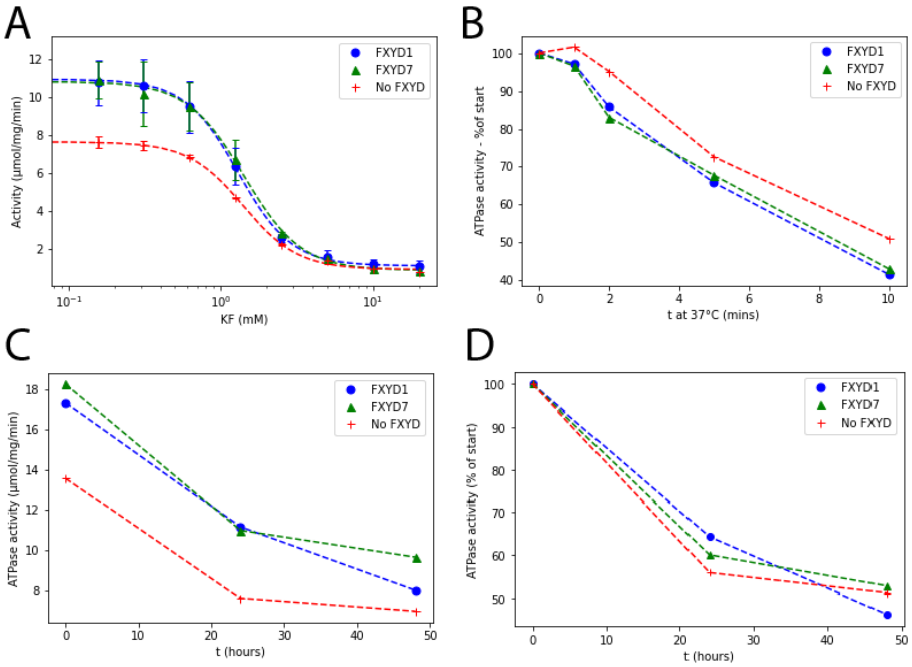

Figure 5 Activity assays of detergent-solubilized α2β2 with FXYD1, FXYD7 and no FXYD. ***A.*** *KF (MgF_x) titration with n=3 (FXYD1: $K_{1/2}$ = 1.30 mM, V_{max} = 10.95 µmol/mg/min, FXYD7: $K_{1/2}$ = 1.42 mM, V_{max} = 10.84 µmol/mg/min, No FXYD: $K_{1/2}$ = 1.40 mM, V_{max} = 7.66 µmol/mg/min).* ***B.*** *Relative decrease of ATPase activity with different FXYDs during incubation at 37°C (n=1). Samples were incubated at 37°C before being placed on ice and subsequently ATPase activity was measured at 37°C.* ***C.*** *Activity decrease of α2β2 over a timeframe of three days. (n=1)* ***D.*** *Relative decrease of activity over three days with regard to the activity at t=0 (n=1).*

Discussion

The Na,K-ATPase has been subjected to a wide range of studies within molecular biology, toxicology, pharmacology, and many other fields of interest. The versatility of this protein enables it to exert its specific function of creating or maintaining an ionic gradient in specialized manners, achieved by variation of subunit isoform combinations. A lot remains to be discovered on the mechanism of how these differences are established. Compared to household isoform α1β1, the combination of α2 with β2 results in a Na,K-ATPase with a low K^+-affinity and high sensitivity to voltage, mainly expressed in heart, skeletal muscle, and astrocytes. Due to its inherent instability, purification has long been a challenge, which posed problematic for structural studies. Here, α2β2 has been expressed in *Pichia pastoris* and reconstituted in Saposin A nanodiscs with the intent of gaining more information on structural characteristics via cryo-EM. Biochemical assays further examined the properties of α2β2 in different environments, mainly comparing purification in KCl with NaCl. Additionally, the effect of FXYD7 on α2β2 has been studied.

Structural analysis of α2β2

It is remarkable that negative stain studies of nanodisc-reconstituted α2β2, purified in high concentration KCl, show a homogenous sample which results in a relatively high-resolution 3D map of the protein. It would be expected that cryo-EM of the same preparation of α2β2 would not differ much regarding the quality of particles, but the dataset did not yield any 2D classes with distinguishable features. Because purification of detergent-solubilized α2β2 in high concentration KCl showed an apparent decrease in stability, the low quality of the cryo-sample would logically be attributed to the fact that it was purified in KCl. However, negative stain data contradicts this in part, suggesting that KCl-purified protein should be of high enough quality to get useful structural data. Nevertheless, KCl concentration might play a bigger role in cryo-EM sample preparation due to the fact that the protein resides in a high concentration KCl environment for a longer time. In another attempt at obtain a useful cryo-EM sample, the high KCl-concentration was replaced with NaCl in the full purification, with a low amount of KCl present to aid transition into an E2 state, stabilized by MgF_x and ATP. An additional change was to add lipids to wash buffers, as to further decrease the time in which the protein is not surrounded by stabilizing lipids. This resulted in a dataset with better looking particles, but still not up to standard with what could be expected from negative stain data. From this, the low quality of the sample may be more so due to other circumstances rather than the presence of KCl.

Therefore, the question arises what the problem could be when producing a sample for cryo-EM. One of the differences between sample preparation of negative stain and cryo-EM is that time plays a factor. The procedure for cryo-EM sample preparation is inherently more time-consuming, as it deals with higher amounts, dialysis, and concentration steps. It is possible that α2β2 destabilizes rather quickly, limiting the time frame in which it is possible to produce grids with high-quality particles. Experimental data of α2β2 incubated with various concentrations of KCl would show whether post-purification incubation with high KCl concentration reduces ATPase compared to samples in NaCl. If there would indeed be a causation between KCl concentration and stability, this could explain the low quality of the first cryo-sample purified in KCl but does not clarify why the mixed NaCl/KCl-purified sample is of insufficient quality.

An additional observation on the cryo-EM datasets of α2β2 was a preferred orientation of the protein. This has not been seen before for samples concerning α1β1 and therefore may be a property specific for α2β2. A wide distribution of particle orientations is essential for useful data processing, as orientation bias leads to a discrepancy in resolution along different axes of the protein. Orientation

bias is generally caused by specific interactions of the protein with the air-water interface. Eliminating this preference was previously solved by adding detergents with a high critical micelle concentration (CMC), such as CHAPSO[73], or by tilting the grid up to 40° during data collection[74]. One of the features that might be important for particle adsorption is the degree of glycosylation, which is highest for the β2-isoform. Therefore, it may be an option to make a sample preparation with deglycosylated α2β2, which might alter the orientation bias.

To understand this difference, it is important to understand how KCl destabilizes α2β2, whether it be because of the mere presence of K^+ or general instability of α2β2 specifically in the E2 state. The latter would explain why α2β2 purified in NaCl/KCl-mixtures but stabilized in E2 by MgF_x and ATP delivers a low quality cryo-EM dataset. Because purification of α2β2 in NaCl seems to yield a more stable protein compared to KCl, this indicates a difference in stability by either i) conformational bias or ii) K- or Na-ion binding. To study this, α2β2 was purified in choline chloride. Since ionic strength stabilizes the Na,K-ATPase in an E1 conformation, a low concentration of KCl was added to induce transition to E2. Stability of α2β2 in this case was improved compared to purification in high KCl, showing that the conformation is not the plausible basis for the stability issues. However, this relatively improved stability of α2β2 does not match the stability of α2β2 when purified in NaCl. Therefore, it is most likely that binding of Na-ions is an important factor in stabilizing α2β2.

The stabilizing effect of Na-ions binding to α2β2 should have a structural explanation. As shown before, α2 Na,K-ATPase can be stabilized by mutations in TM helices M8-M10, by increasing interactions between the protein and phosphatidylserine (PS)[72], stabilizing the protein comparable to α1. The importance of phosphatidylserine and cholesterol for the stability of the Na,K-ATPase has been proven extensively[45,75–77]. Although movement of TM helices 8-10 have not directly been observed in structures to date, M8 residues have been observed to be of importance to binding of Na^+ [78], which may enhance interactions with PS and/or cholesterol for α2β2. It is important to note that destabilization of α2β2 ATPase activity has been observed in detergent, providing a different, perhaps less stable, lipid environment for the protein. Therefore, observed destabilization in detergent may not be fully transferable to aggregation of any reconstituted samples, as is the case for cryo-EM and negative stain.

To disclose any effects on instability, experiments should determine the nature of the problem. It may be wise to focus on the difference between KCl and NaCl in detergent-solubilized α2β2. Because ATPase activity does not necessarily represent protein stability, assays specifically designed to measure protein stability might provide more information, e.g. Circular Dichroism Spectroscopy. To accurately determine the effect of both KCl and NaCl, purification should be performed in varying amounts of both salts. To further accurately determine the correlation of KCl concentration with stability, it is also important to know in what stage it has a destabilizing effect, whether it be during purification or also after purification/reconstitution. Therefore, these incubations with KCl might provide more insight on this mechanism. More insight into molecular differences when transitioning between states can also be of use when studying the difference in stability. Dynamics of transmembrane segments can be monitored with Single-molecule Fluorescence Resonance Energy Transfer (Sm-FRET)[79]s, which might help to understand the intermolecular movements that cause the instability and whether this relates to with protein-lipid interactions. If transition into an E2 state differs in α2 compared to other alpha isoforms, Sm-FRET can determine differences in distances between transmembrane helices.

Ultimately, the goal is to be able to analyse the structure of α2β2, which seems relatively feasible from the negative stain data provided in this study. Alterations to the purification procedure or grid preparation are necessary to produce a useful sample for cryo-EM. The addition of lipids during

washes seemed to help elevate the quality of the sample, but not nearly enough to conclude any structural details from. Stabilization of α2β2 by MgF_x and ATP, entrapping it in an E2 state, could be an issue for the stability of the protein, therefore it could be advantageous to explore other stabilizing molecules, including metal fluorides and cardiotonic steroids.

Stability of α2β2 with FXYD7

Considered an accessory subunit of the Na,K-ATPase, FXYD proteins are usually not the centre of attention in studies concerning the protein. However, they do play a regulatory role, which can be important for the tissue-specific functions of the Na,K-ATPase[80]. Since addition of FXYD to the Na,K-ATPase strongly stabilizes the protein[45,81], possibly because of its involvement in PS/cholesterol interaction, they are of specific interest for α2. A recent study mapping crosslinks of synaptic interactions by mass spectrometry showed that there might be a possible preference of α2 to interact with FXYD7 in the brain[60]. An earlier study, however, concluded no association of FXYD7 to α2 in the brain and no interaction of αβ2 with FXYD7 in *Xenopus* oocytes[59]. For α1β1 complexes that did associate with FXYD7, the K^+-affinity was lowered[82]. Therefore, if FXYD7 would associate with α2β2 in the brain, its effect would be in accordance with the presumed function of α2β2 in astrocytes, if it acts in the same way as with α1β1 complexes. In this study, FXYD1 was used for most purifications of α2β2. To follow up on the stability issues, the effect of FXYD7 on the stability of α2β2 was studies by means of ATPase activity assays. The activity was monitored after short incubations at 37 °C or over long time periods on ice.

The general conclusion that could be drawn from the preliminary data regarding stability comparison of FXYD7 to FXYD1, is that FXYD7 stabilizes α2β2 in the same manner as FXYD1 during purification but stability of ATPase activity is independent of any FXYD after purification. However, there are some factors that should be considered when interpreting these data. Firstly, purification for these assays was done in detergent, meaning that the lipidic environment of α2β2 is less stable and further from native conditions compared to lipid bilayers created with liposomes or nanodiscs. As mentioned before, FXYD proteins are involved in establishing the stabilizing interactions with PS and cholesterol. Therefore, the fact that measurements are done in detergent might complicate how lipids interact with the protein following the flexible lipid environment. Given the discrepancy in structural studies regarding the stability of α2β2, the stability of detergent-solubilized Na,K-ATPase does not necessarily reflect the stability of α2β2 in Saposin. However, any strong differences in stabilizing effects of FXYD1 and FXYD7 should be indicative of any change in the protein complex. Additional experiments should be done to confirm the observed data, especially since results are not statistically supported. With this in mind, stability assays of nanodisc reconstituted α2β2 with varying FXYD's may provide more accurate insights into any difference in stability.

Although it would be advantageous if FXYD7 provided a stabilizing effect to α2β2, any difference in stabilizing effects between FXYD's has not been observed before. Post translational modifications of FXYD proteins, such as palmitoylation, have been suggested to play a role in membrane stabilization[43], but palmitoylation has mainly been assigned a regulatory role since it diminishes the effect of FXYD1 on ion-affinities[83]. For FXYD7, a major posttranslational modification that has been identified is O-glycosylation of three N-terminal threonine residues[84]. O-glycosylation of FXYD7 is important for its stability, but it has also been found that FXYD7 can, independently of αβ-coexpression, be translocated to the membrane because of this post-translational modification[85]i. Whether the stabilization extends towards stabilization of the αβ-complex is not known. The fact that FXYD7 can dissociate from the endoplasmic reticulum on itself might explain why it was initially not found to be interacting with α2-complexes, as association was assessed in oocyte microsomes. Because of this, studies of α2 and FXYD7 have remained absent, thus, the effect of FXYD7 on α2 is not yet disclosed, especially since it

already has been found to exert a different effect depending on the α-isoform. Therefore, any experiments judging ion-affinity changes may provide new insights into the importance of regulation by FXYD7 in the brain. Next to this, expression and association of FXYD7 and α2β-complexes should be considered, since the ability of independent translocation of FXYD7 fits the short-term reaction necessity of α2β to react to fast ion gradient changes.

Conclusion

The Na,K-ATPase isoform complex α2β2 was successfully purified and reconstituted in Saposin A nanodiscs in this study, after which structural studies were done using (cryo-)electron microscopy. Although initial analysis provided a promising outlook, cryo-EM sample preparation should be optimized in order to obtain a useful dataset for structure determination. In the future, additional directions may provide more information, such as variation of conformations by using different stabilizing agents including cardiotonic steroids or studying different isoform combinations such as α2β1. Additionally, FXYD7 was found to stabilize α2β2 during purification in the same fashion as FXYD1, although more data is needed to confirm this notion. FXYD7 may also be of interest to different isoforms, e.g. the neuronal α3, further providing information on the effect of FXYD7 on the Na,K-ATPase. In conclusion, structural analysis of the α2β2 isoform of the Na,K-ATPase is a promising direction to gain insights into the overall mechanism of the protein and FXYD7 may also be a subject of interest with regard to its regulatory and stabilizing role.

References

1. Mulkidjanian, A. Y., Bychkov, A. Y., Dibrova, D. V., Galperin, M. Y. & Koonin, E. V. Origin of first cells at terrestrial, anoxic geothermal fields. *Proc. Natl. Acad. Sci. U. S. A.* **109**, (2012).

2. Skou, J. C. The influence of some cations on an adenosine triphosphatase from peripheral nerves. *BBA - Biochim. Biophys. Acta* **23**, 394–401 (1957).

3. Nicholls, M. Jens Christian Skou. *Eur. Heart J.* **40**, 3281–3283 (2019).

4. Clausen, M. V., Hilbers, F. & Poulsen, H. The structure and function of the Na,K-ATPase isoforms in health and disease. *Front. Physiol.* **8**, 1–16 (2017).

5. El Mernissi, G. & Doucet, A. Quantitation of [3H]ouabain binding and turnover of Na-K-ATPase along the rabbit nephron. *Am. J. Physiol. - Ren. Fluid Electrolyte Physiol.* **16**, (1984).

6. Harris, J. J., Jolivet, R. & Attwell, D. Synaptic Energy Use and Supply. *Neuron* **75**, 762–777 (2012).

7. Schwinger, R. H. G. *et al.* Reduced sodium pump α1, α3, and β1-isoform protein levels and Na+, K+-ATPase activity but unchanged Na+-Ca2+ exchanger protein levels in human heart failure. *Circulation* **99**, 2105–2112 (1999).

8. Yuan, S. & Joseph, E. M. The small heart mutation reveals novel roles of Na+/K +-ATPase in maintaining ventricular cardiomyocyte morphology and viability in zebrafish. *Circ. Res.* **95**, 595–603 (2004).

9. Sweadner, K. J. *et al.* Genotype-structure-phenotype relationships diverge in paralogs ATP1A1, ATP1A2, and ATP1A3. *Neurol. Genet.* **5**, (2019).

10. De Carvalho Aguiar, P. *et al.* Mutations in the Na+/K+-ATPase α3 gene ATP1A3 are associated with rapid-onset dystonia parkinsonism. *Neuron* **43**, 169–175 (2004).

11. Ohnishi, T. *et al.* Na, K-ATPase α3 is a death target of Alzheimer patient amyloid-β assembly. *Proc. Natl. Acad. Sci. U. S. A.* **112**, E4465–E4474 (2015).

12. Shrivastava, A. N. *et al.* a-synuclein assemblies sequester neuronal a3-Na+/ K+-ATPase and impair Na+ gradient. **34**, 2408–2423 (2015).

13. De Fusco, M. *et al.* Haploinsufficiency of ATP1A2 encoding the Na+/K+ pump α2 subunit associated with familial hemiplegic migraine type 2. *Nat. Genet.* **33**, 192–196 (2003).

14. Schatzmann HJ, R. B. Hemmung des aktiven Na-K-Transports und der Na+K-aktivierten Membran-ATPase von Erythrocytenstromata durch Ouabain [Inhibition of the active Na-K-transport and Na-K-activated membrane ATP-ase of erythrocyte stroma by ouabain]. *Helv Physiol Pharmacol Acta.* **65**, (1965).

15. Ziff, O. J. & Kotecha, D. Digoxin: The good and the bad. *Trends Cardiovasc. Med.* **26**, 585–595 (2016).

16. Ayogu, J. I. & Odoh, A. S. Prospects and Therapeutic Applications of Cardiac Glycosides in Cancer Remediation. *ACS Comb. Sci.* **22**, 543–553 (2020).

17. Palmgren, M. G. & Nissen, P. P-Type ATPases. *Annu. Rev. Biophys.* **40**, 243–266 (2011).

18. Geering, K. The functional role of β subunits in oligomeric P-type ATPases. *J. Bioenerg. Biomembr.* **33**, 425–438 (2001).

19. Blanco, G. Na,K-ATPase subunit heterogeneity as a mechanism for tissue-specific ion

regulation. *Semin. Nephrol.* **25**, 292–303 (2005).

20. Laursen, M., Gregersen, J. L., Yatime, L., Nissen, P. & Fedosova, N. U. Structures and characterization of digoxin- And bufalin-bound Na+,K+-ATPase compared with the ouabain-bound complex. *Proc. Natl. Acad. Sci. U. S. A.* **112**, 1755–1760 (2015).

21. Gadsby, D. C., Bezanilla, F., Rakowski, R. F., De Weer, P. & Holmgren, M. The dynamic relationships between the three events that release individual Na+ ions from the Na+/K+-ATPase. *Nat. Commun.* **3**, 666–669 (2012).

22. Post, R. L., Hegyvary, C. & Kume, S. Activation by Adenosine Triphosphate in the Phosphorylation Kinetics of Sodium and Potassium Ion Transport Adenosine Triphosphatase. *J. Biol. Chem.* **247**, 6530–6540 (1972).

23. Albers, R. W. Biochemical aspects of active transport. *Annu. Rev. Biochem.* **36**, 727–756 (1967).

24. Poulsen, H. *et al.* Neurological disease mutations compromise a γ-terminal ion pathway in the Na+/K+-ATPase. *Nature* **467**, 99–102 (2010).

25. Shrivastava, A. N., Triller, A. & Melki, R. Cell biology and dynamics of Neuronal Na+/K+-ATPase in health and diseases. *Neuropharmacology* **169**, 107461 (2020).

26. Dostanic, I., Schultz, J. E. J., Lorenz, J. N. & Lingrel, J. B. The α1 isoform of Na,K-ATPase regulates cardiac contractility and functionally interacts and co-localizes with the Na/Ca exchanger in heart. *J. Biol. Chem.* **279**, 54053–54061 (2004).

27. Nishimoto, K. *et al.* Aldosterone-stimulating somatic gene mutations are common in normal adrenal glands. *Proc. Natl. Acad. Sci. U. S. A.* **112**, E4591–E4599 (2015).

28. Watts, A. G., Sanchez-Watts, G., Emanuel, J. R. & Levenson, R. Cell-specific expression of mRNAs encoding Na+,K+-ATPase α- and β-subunit isoforms within the rat central nervous system. *Proc. Natl. Acad. Sci. U. S. A.* **88**, 7425–7429 (1991).

29. Sweadner, K. J. *et al.* Immunologic identification of Na+,K+-ATPase isoforms in myocardium: Isoform change in deoxycorticosterone acetate-salt hypertension. *Circ. Res.* **74**, 669–678 (1994).

30. Bøttger, P. *et al.* Distribution of Na/K-ATPase alpha 3 isoform, a sodium-potassium P-type pump associated with rapid-onset of dystonia parkinsonism (RDP) in the adult mouse brain. *J. Comp. Neurol.* **519**, 376–404 (2011).

31. Blanco, G., Sanchez, G., Melton, R. J., Tourtellotte, W. G. & Mercer, R. W. The α4 isoform of the Na,K-ATPase is expressed in the germ cells of the testes. *J. Histochem. Cytochem.* **48**, 1023–1032 (2000).

32. Woo, A. L., James, P. F. & Lingrel, J. B. Characterization of the fourth α isoform of the Na,K-ATPase. *J. Membr. Biol.* **169**, 39–44 (1999).

33. Habeck, M. *et al.* Selective assembly of Na,K-ATPase α2 β2 Heterodimers in the Heart: Distinct functional properties and isoform-selective inhibitors. *J. Biol. Chem.* **291**, 23159–23174 (2016).

34. Tokhtaeva, E., Clifford, R. J., Kaplan, J. H., Sachs, G. & Vagin, O. Subunit isoform selectivity in assembly of Na,K-ATPase α-β heterodimers. *J. Biol. Chem.* **287**, 26115–26125 (2012).

35. Crambert, G. *et al.* Transport and pharmacological properties of nine different human Na,K-ATPase isozymes. *J. Biol. Chem.* **275**, 1976–1986 (2000).

36. Kirley, T. L. Determination of three disulfide bonds and one free sulfhydryl in the β subunit of (Na,K)-ATPase. *J. Biol. Chem.* **264**, 7185–7192 (1989).

37. Roy, M., Sivan-Loukianova, E. & Eberl, D. F. Cell-type-specific roles of Na+/K+ ATPase subunits in Drosophila auditory mechanosensation. *Proc. Natl. Acad. Sci. U. S. A.* **110**, 181–186 (2013).

38. Magyar, J. P. *et al.* Degeneration of neural cells in the central nervous system of mice deficient in the gene for the adhesion molecule on glia, the β2 subunit of murine Na,K-ATPase. *J. Cell Biol.* **127**, 835–845 (1994).

39. Hilbers, F. *et al.* Tuning of the Na,K-ATPase by the beta subunit. *Sci. Rep.* **6**, (2016).

40. Senner, V. *et al.* AMOG/β2 and glioma invasion: Does loss of AMOG make tumour cells run amok? *Neuropathol. Appl. Neurobiol.* **29**, 370–377 (2003).

41. Juel, C., Hostrup, M. & Bangsbo, J. The effect of exercise and beta2-adrenergic stimulation on glutathionylation and function of the Na,K-ATPase in human skeletal muscle. *Physiol. Rep.* **3**, (2015).

42. Geering, K. Function of FXYD proteins, regulators of Na,K-ATPase. *J. Bioenerg. Biomembr.* **37**, 387–392 (2005).

43. Meyer, D. J. *et al.* FXYD protein isoforms differentially modulate human Na/K pump function. *J. Gen. Physiol.* **152**, (2020).

44. Meij, I. C. *et al.* Dominant isolated renal magnesium loss is caused by misrouting of the Na+,K+-ATPase γ-subunit. *Ann. N. Y. Acad. Sci.* **986**, 437–443 (2003).

45. Lifshitz, Y. *et al.* Purification of the human α2 isoform of Na,K-ATPase expressed in Pichia pastoris. Stabilization by lipids and FXYD1. *Biochemistry* **46**, 14937–14950 (2007).

46. Larsen, B. R. *et al.* Contributions of the Na+/K+-ATPase, NKCC1, and Kir4.1 to hippocampal K+ clearance and volume responses. *Glia* **62**, 608–622 (2014).

47. Lauritzen, M. *et al.* Clinical relevance of cortical spreading depression in neurological disorders: Migraine, malignant stroke, subarachnoid and intracranial hemorrhage, and traumatic brain injury. *J. Cereb. Blood Flow Metab.* **31**, 17–35 (2011).

48. Bøttger, P. *et al.* Glutamate-system defects behind psychiatric manifestations in a familial hemiplegic migraine type 2 disease-mutation mouse model. *Sci. Rep.* **6**, 1–21 (2016).

49. Capuani, C. *et al.* Defective glutamate and K + clearance by cortical astrocytes in familial hemiplegic migraine type 2 . *EMBO Mol. Med.* **8**, 967–986 (2016).

50. Morth, J. P. *et al.* Crystal structure of the sodium-potassium pump. *Nature* **450**, 1043–1049 (2007).

51. Laursen, M., Yatime, L., Nissen, P. & Fedosova, N. U. Crystal structure of the high-affinity Na+,K+-ATPase- ouabain complex with Mg2+ bound in the cation binding site. *Proc. Natl. Acad. Sci. U. S. A.* **110**, 10958–10963 (2013).

52. Nyblom, M. *et al.* Crystal structure of Na+, K+-ATPase in the Na +-bound state. *Science (80-.).* **342**, 123–127 (2013).

53. Shinoda, T., Ogawa, H., Cornelius, F. & Toyoshima, C. Crystal structure of the sodium-potassium pump at 2.4 resolution. *Nature* **459**, 446–450 (2009).

54. Ogawa, H., Shinoda, T., Cornelius, F. & Toyoshima, C. Crystal structure of the sodium-potassium pump (Na+,K +-ATPase) with bound potassium and ouabain. *Proc. Natl. Acad. Sci.*

U. S. A. **106**, 13742–13747 (2009).

55. Ogawa, H., Cornelius, F., Hirata, A. & Toyoshima, C. Sequential substitution of K+ bound to Na+,K+-ATPase visualized by X-ray crystallography. *Nat. Commun.* **6**, 1–9 (2015).

56. Toyoshima, C. Structural aspects of ion pumping by Ca2+-ATPase of sarcoplasmic reticulum. *Arch. Biochem. Biophys.* **476**, 3–11 (2008).

57. Winther, A. M. L. *et al.* The sarcolipin-bound calcium pump stabilizes calcium sites exposed to the cytoplasm. *Nature* **495**, 265–269 (2013).

58. Rawson, S., Davies, S., Lippiat, J. D. & Muench, S. P. The changing landscape of membrane protein structural biology through developments in electron microscopy. *Mol. Membr. Biol.* **33**, 12–22 (2016).

59. Béguin, P. *et al.* FXYD7 is a brain-specific regulator of Na, K-ATPase α1-β isozymes. *EMBO J.* **21**, 3264–3273 (2002).

60. Gonzalez-Lozano, M. A. *et al.* Stitching the synapse: Cross-linking mass spectrometry into resolving synaptic protein interactions. *Sci. Adv.* **6**, 1–15 (2020).

61. Byrne, B. Pichia pastoris as an expression host for membrane protein structural biology. *Curr. Opin. Struct. Biol.* **32**, 9–17 (2015).

62. Cregg, J. M., Cereghino, J. L., Shi, J. & Higgins, D. R. Recombinant protein expression in Pichia pastoris. *Appl. Biochem. Biotechnol. - Part B Mol. Biotechnol.* **16**, 23–52 (2000).

63. Allais, J. J., Louktibi, A. & Baratti, J. Oxidation of Methanol by the Yeast, Pichia pastoris, Purification and Properties of the Formaldehyde Dehydrogenase. *Agric. Biol. Chem.* **47**, 1509–1516 (1983).

64. Borch, J. & Hamann, T. The nanodisc: A novel tool for membrane protein studies. *Biol. Chem.* **390**, 805–814 (2009).

65. Rouck, J. E., Krapf, J. E., Roy, J., Huff, H. C. & Das, A. Recent advances in nanodisc technology for membrane protein studies (2012–2017). *FEBS Lett.* **591**, 2057–2088 (2017).

66. Bayburt, T. H., Sligar, S. G. & Biology, C. Membrane protein assembly into nanodiscs. **584**, 1721–1727 (2016).

67. Denisov, I. G. & Sligar, S. G. Nanodiscs for structural and functional studies of membrane proteins. *Nat. Struct. Mol. Biol.* **23**, 481–486 (2016).

68. Frauenfeld, J. *et al.* A saposin-lipoprotein nanoparticle system for membrane proteins. *Nat. Methods* **13**, 345–351 (2016).

69. Carragher, B. *et al.* Leginon: An automated system for acquisition of images from vitreous ice specimens. *J. Struct. Biol.* **132**, 33–45 (2000).

70. Grant, T., Rohou, A. & Grigorieff, N. cisTEM, user-friendly software for single- particle image processing. *Elife* **7**, 1–24 (2018).

71. Punjani, A., Rubinstein, J. L., Fleet, D. J. & Brubaker, M. A. CryoSPARC: Algorithms for rapid unsupervised cryo-EM structure determination. *Nat. Methods* **14**, 290–296 (2017).

72. Kapri-Pardes, E. *et al.* Stabilization of the α2 isoform of Na,K-ATPase by mutations in a phospholipid binding pocket. *J. Biol. Chem.* **286**, 42888–42899 (2011).

73. Kampjut, D., Steiner, J. & Sazanov, L. A. Cryo-EM grid optimisation for membrane proteins.

iScience **24**, 102139 (2021).

74. Chen, J., Noble, A. J., Kang, J. Y. & Darst, S. A. Eliminating effects of particle adsorption to the air/water interface in single-particle cryo-electron microscopy: Bacterial RNA polymerase and CHAPSO. *J. Struct. Biol. X* **1**, 100005 (2019).

75. Habeck, M. *et al.* Stimulation, inhibition, or stabilization of Na,K-ATPase caused by specific lipid interactions at distinct sites. *J. Biol. Chem.* **290**, 4829–4842 (2015).

76. Habeck, M., Kapri-Pardes, E., Sharon, M. & Karlish, S. J. D. Specific phospholipid binding to Na,K-ATPase at two distinct sites. *Proc. Natl. Acad. Sci. U. S. A.* **114**, 2904–2909 (2017).

77. Cornelius, F., Habeck, M., Kanai, R., Toyoshima, C. & Karlish, S. J. D. General and specific lipid-protein interactions in Na,K-ATPase. *Biochim. Biophys. Acta - Biomembr.* **1848**, 1729–1743 (2015).

78. Imagawa, T., Yamamoto, T., Kaya, S., Sakaguchi, K. & Taniguchi, K. Thr-774 (transmembrane segment M5), Val-920 (M8), and Glu-954 (M9) are involved in Na+ transport, and Gln-923 (M8) is essential for Na,K-ATPase activity. *J. Biol. Chem.* **280**, 18736–18744 (2005).

79. Mazal, H. & Haran, G. Single-molecule FRET methods to study the dynamics of proteins at work. *Curr. Opin. Biomed. Eng.* **12**, 8–17 (2019).

80. Geering, K. FXYD proteins: New regulators of Na-K-ATPase. *Am. J. Physiol. - Ren. Physiol.* **290**, (2006).

81. Haviv, H. *et al.* Stabilization of Na+,K+-ATPase purified from Pichia pastoris membranes by specific interactions with lipids. *Biochemistry* **46**, 12855–12867 (2007).

82. Li, C. *et al.* Structural and functional interaction sites between Na,K-ATPase and FXYD proteins. *J. Biol. Chem.* **279**, 38895–38902 (2004).

83. Tulloch, L. B. *et al.* The inhibitory effect of phospholemman on the sodium pump requires its palmitoylation. *J. Biol. Chem.* **286**, 36020–36031 (2011).

84. Crambert, G. *et al.* FXYD7, the First Brain- and Isoform-specific Regulator of Na,K-ATPase. *Annu. New York Acad. Sci.* **986**, 444–448 (2003).

85. Moshitzky, S., Asher, C. & Garty, H. Intracellular Trafficking of FXYD1 (Phospholemman) and FXYD7 Proteins in Xenopus Oocytes and Mammalian Cells *. *J. Biol. Chem.* **287**, 21130–21141 (2012).